IL-27 neutralization to modulate the tumor microenvironment and increase immune checkpoint immunotherapy efficacy

Loukas Papargyris[1*], Quentin Glaziou[2*], Laetitia Basset[3], Sènan d'Almeida[4], Pascale Pignon[5], Nabila Jabrane-Ferrat[2], Christophe Blanquart[6], Yves Delneste[7], Julie Tabiasco[2]

[1] Department of Infectious Disease, Imperial College London, London, UK

[2] Toulouse Institute for Infectious and Inflammatory Diseases (INFINITy), INSERM, CNRS, Toulouse III Paul Sabatier University, Toulouse, France

[3] Department of Pathology, University Hospital of Angers, Angers, Université d'Angers, Inserm UMR 1307, CNRS UMR 6075, Nantes Université, CRCI2NA, 49000, Angers, France.

[4] Viollier AG, Allschwil 4123, Switzerland

[5] Univ Angers, Nantes Université, INSERM, CNRS, CRCI2NA, SFR ICAT, Angers, France

[6] Nantes Université, Inserm UMR 1307, CNRS UMR 6075, Université d'Angers, CRCI2NA, F-44000 Nantes, France.

[7] Univ Angers, Nantes Université, INSERM, CNRS, CRCI2NA, SFR ICAT, Angers, France; University Hospital of Angers, Angers, France

* LP and QG contributed equally to this study

Abstract

Tumor-associated macrophages (TAMs) accumulate in the majority of solid tumors, producing inflammatory cytokines and growth factors involved in tumor maintenance. They have recently emerged as targets for restoring an effective antitumor response and limiting tumor growth. In the present study, we investigated the potential of IL-27 neutralization to modify macrophage polarization and thus the tumor immune microenvironment.

We monitored the effect of IL-27 neutralization on human macrophages and in vivo in a murine colon adenocarcinoma model.

In this study, we demonstrated the importance of IL-27 in the generation of human immunoregulatory macrophages. Mechanistically, IL-27 neutralization reduced the immunosuppressive properties of macrophages. These modifications led to a reduction in the ability of macrophages to inhibit the function of $CD4^+$ and $CD8^+$ T cells. Furthermore, in vivo neutralization of IL-27 reduced MC38 tumor growth.

Collectively, we uncovered the role of IL-27 in the immunosuppressive tumor microenvironment. IL-27 neutralization thus appears as a promising strategy to target macrophages in immunosuppressive TME and improve the clinical efficacy of immunotherapy protocols.

Keywords

Tumor Microenvironment, Immunotherapy, Macrophages, Immune Checkpoint, IL-27

Introduction

Resistance to ICIs currently used in antitumor therapy, may develop due to a variety of reasons, including the accumulation of immunosuppressive factors in the tumor microenvironment (TME) [1], like the upregulation of other immune checkpoints such.[2]

In established tumors, TME mainly contains immunosuppressive cells and numerous immunosuppressive mediators such as cytokines, chemokines, prostaglandin or adenosine.[3,4] Modulating the TME appears to be therapeutically promising, but the multiplicity of pro-tumoral factors in the TME makes this an almost unachievable goal.[4] A challenging but feasible approach is to directly target immune cells in the TME and try to re-educate them toward a more antitumoral status.

Macrophages in cancer, known as tumor-associated macrophages (TAMs), are the most abundant immune cells in solid tumors and are associated with poor prognosis.[5,6] TAMs exhibit a high degree of functional heterogeneity, displaying pro- and anti-inflammatory functions depending on their surrounding tissue microenvironment.[6,7] In established tumors, TAMs display an immunoregulatory phenotype that promotes tumor growth by producing proangiogenic and trophic factors, and by inducing the recruitment and polarization of monocytes and other immune cells toward a regulatory phenotype via soluble mediator and membrane molecule expression.[6,8]

Recent studies on various solid-tumor models suggest that preventing macrophage accumulation or activation in tumors may be a potential therapeutic option.[9–11] However, the reversion of the immunosuppressive phenotype of macrophages may be mechanistically more effective.[9,11–15]

We and others have previously shown that CD39 expression and IL-10 secretion are highly dependent on interleukin 27 (IL-27), an immunoregulatory cytokine shown to modulate inflammation through a series of mechanisms.[16–18] In vitro and in vivo experiments have demonstrated that IL-27 enhances the expression of multiple co-inhibitory molecules, including CD39, on tumor cells and T cells.[19,20]

In this work, we show the impact of IL-27 neutralization on the phenotype, metabolism and function of human immunoregulatory macrophages and highlight the therapeutic interest of clinically targeting IL-27 to improve the immune response and to enhance the efficacy of approved or novel ICI treatments against cancer.

Material and Methods

Fully detailed methods are described in supplemental materials parts

Cell culture

$CD4^+$ and $CD8^+$ T cells and $CD14^+$ monocytes were isolated from healthy donor mononuclear cells (agreement ANG-2003-2) by positive magnetic sorting (Miltenyi Biotec, Germany). Macrophages were generated by culturing monocytes for 7 days with 50 ng/ml M-CSF or 50 ng/ml GM-CSF (ORF Genetics Kopavogur, Iceland). IL-27-neutralizing antibody (5 µg/mL) or isotype control antibody (5 µg/mL) (both R&D Systems, Abingdon, UK) were added in the monocyte cultures (Day 0 and Day 3) to generate Mα27 and Miso, respectively. Caffeine (Sigma-Aldrich, St. Louis, USA) or the EP2 inhibitor AH6809 (Cayman Chemical Company, Michigan, USA) were added in cultures.

Cell activation

Macrophages were plated at $2x10^5$ cells per well and activated with 200 ng/mL LPS (serotype E. coli O111: B4; Sigma-Aldrich). Purified $CD4^+$ or $CD8^+$ T cells were plated at $2x10^5$ cells per well and stimulated with PHA at 10 µg/mL (Sigma-Aldrich, St. Louis, MO).

Culture supernatants were collected after 48 h and frozen at -80°C.

For transcriptomic analysis, cells were collected after 6 h, suspended in Trizol reagent (Life technologies, Saint Aubin, France) and stored at -80°C.

For $CD4^+$ T cell proliferation assay, $CD4^+$ T cells, previously incubated with 3µM CFDA-SE (Molecular Probes, Carlsbad, CA), were cultured in flat-bottom 96-well plates pre-coated with 1 µg/mL anti-CD3 antibody (clone OKT3; ATCC, Manassas, VA) in supplemented RPMI media containing 1 µg/mL soluble anti-CD28 antibody (BD Pharmingen) with or without 50% volume of activated macrophage supernatant. After 6 days, $CD4^+$ T cell proliferation was measured by flow cytometry using CFDA-SE dilution analysis.

For $CD8^+$ T cell cytotoxicity assay, co-cultures of 10^5 Muc1-specific $CD8^+$ T cells[21] and $3x10^4$ Meso34 (tumor cells overexpressing muc-1 and expressing the luciferase enzyme) were incubated for 72 h with or without $2x10^4$ macrophages. Quantification of luciferase in culture supernatants was carried out by measuring photon emission induced after addition of the luciferase substrate coelenterazine (Interchim, Montluçon, France), with a CLARIOstar Plus reader (BMG Labtech, Ortenberg, Germany).

Tumor model

After 2 weeks quarantine following arrival8-week old female C57BL/6J mice (Janvier, France) were injected subcutaneously in the right flank with $5x10^5$ MC38 murine colon tumor cell line suspended in 100 µL PBS. As soon as tumors were detectable in all mice (about 8-10 days after injection), they were randomly divided into two groups and one group was treated with IL-27-neutralizing antibody (Anti-mouse IL-27p28, Clone: MM27-7B1, Ultra LEAF purified; Biolegend) and the other with a non-relevant control antibody of the same isotype (Biolegend), every 48 h. Treatment was injected five times intratumorally at 20 µg/20 µL/injection.

Treatment with anti-PD-L1 antibody (Anti-mouse PD-L1, Clone: 10F.9G2, InVivoMab, Bioxcell) was started two days after the end of treatment with anti-IL-27 antibody and administered to mice by intraperitoneal injection (200 µg/200 µl/injection) every three days. Tumor growth was monitored at the time of the first injection then every two days. Tumor volume was calculated using the formula: tumor volume = (tumor length x tumor width x tumor height) x 0.52. Mice were euthanized when a tumor volume reaches a maximum of 1800 mm3. The measurements were always made by two people at the same time, one of whom knew the treatment. The number of mice used in each experiment was calculated by a power calculation depending on the magnitude of the effect observed in preliminary experiments.

Statistics

GraphPad Prism 10 was used for all statistical analyses.

Results

IL-27 neutralization during immunosuppressive macrophages differentiation leads to a reduction in their immunosuppressive properties.

To define the impact of IL-27 neutralization on macrophages, we characterized their phenotypic changes after treatment. We used macrophages representative of the immunoregulatory ones found in tumors. [22] They were obtained by culturing monocytes, in the presence of M-CSF for 7 days (M-CSF macrophages). In order to neutralize IL-27, we added an IL-27 blocking antibody (α IL-27 Ab) or a

control antibody of the same isotype (control Ab) during the seven days of cell differentiation.

We first confirmed that IL-27 neutralization reduced the membrane and mRNA expression of CD39 in the resulting macrophages (Mα27) compared to macrophages cultured in the presence of control antibody (Miso).[17]

Adenosine is an immunomodulator molecule involved in the acquisition of immunoregulatory properties by macrophages, including increased expression of CD39.[23] Addition of caffeine, a non-selective adenosine receptor antagonist, during macrophage differentiation, resulted in significantly decreased CD39 expression (Supplementary Figure 1A). Also, we defined the impact of IL-27 neutralization on the expression of CD73, the main enzyme catalyzing the conversion of AMP to adenosine on the surface of immune cells. We found significantly decreased expression of CD73 on differentiated Mα27 macrophages compared to the Miso ones (Figure 1A and B). This result is consistent with the significant decrease of CD73 mRNA levels in Mα27 compared to Miso (Supplementary Figure 2A).

We have previously shown that IL-27 neutralization led to a reduction in PD-L1 expression on Mα27 compared to Miso.[17] To further investigate the expression of immunoregulatory molecules by anti-IL-27-treated macrophages, we looked at CD155, an emerging immune control molecule that has now become an important target for immunotherapy.[24–27] We observed a significant decrease of CD155 expression on Mα27 compared to Miso, of around 25% (Figure 1C).

CD80 is a major costimulatory molecule that activates effector cells described in the literature as specifically expressed by pro-inflammatory macrophages and as a prognostic marker in several cancers.[28] CD40, a member of the tumor necrosis factor receptor family, is an activator for macrophages expressing it, that also induces the activation of T cells expressing CD40L.[29] Compared to Miso cells, Mα27 have significantly increased their CD80 (Figure 1D) and CD40 (Figure 1E) expression by about 67% and 68%, respectively, at the end of differentiation. Furthermore, we found that differentiated Mα27 exhibit increased expression of the CD48 molecule, an activating receptor for the cells expressing it, compared to Miso (Figure 1F). Macrophages are also known to produce soluble mediators based on their activation and differentiation status that is defined by the TME. Chemokines like CCL2 and CCL22 and mediators like PGE2 and GM-CSF contribute to the recruitment and polarization of monocytes and other immune cells in the TME. CCL2 enables the recruitment of monocytes that differentiate locally

into immunoregulatory macrophages under the influence of the TME. We found that, Mα27 at steady state secrete significantly less CCL2 than Miso (Figure 1G) and more after activation (Supplementary Figure 2B). This secretion profile appears to be comparable to the profile of the inflammatory macrophage, with higher CCL2 secretion after TLR engagement as compared to the resting state. CCL22 is known to recruit $CCR4^{+}$ regulatory T cells into the TME.[4] We observed here that Mα27 secreted significantly less CCL22 than Miso (Figure 1H).

We have previously described that IL-27 neutralization lead to a significant decrease in IL-10 secretion by activated Mα27 compared to Miso[17]; we confirmed this finding here (Supplementary Figure 2C).

PGE2 is involved in the acquisition of immunoregulatory properties in M-CSF-differentiated macrophages.[30] Supplementary figure 1B shows that PGE2 controls the CD39 expression, its inhibition during M-CSF-mediated macrophage differentiation significantly decreased the level of CD39 expression.

We further found that differentiated Mα27 secrete significantly less PGE2 than Miso (Figure 1I). This result can be explained by the significant decrease of mRNA (Supplementary Figure 2D) and protein (Supplementary Figure 2E and F) levels of cyclooxygenase-2 (COX-2), also known as prostaglandin-endoperoxide synthase 2 (PTGS2), the enzyme which catalyzes the biochemical cascade that converts the arachidonic acid into prostaglandin.

We showed that a low concentration of GM-CSF added during macrophage differentiation with M-CSF led to a drastic loss of CD39 expression (Supplementary Figure 1C) conferring pro-inflammatory properties to macrophages.[31] GM-CSF is currently being studied to modulate the TME and preclinical research in numerous cancer models has shown that GM-CSF acts on dendritic cells (DC) in a way that may promote long-term antitumor immune responses, prompting clinical trials for testing the use of recombinant GM-CSF in cancer.[15] We found that Mα27 secreted significantly more GM-CSF than Miso (Figure 1J).

These results suggest that the decreased expression of immunoregulatory molecules CD39, CD73, CD155, COX-2 and production of IL-10, CCL2, CCL22 and PGE2, combined with an increase in secretion of GM-CSF and expression of immunostimulatory molecules like CD80, CD40 and CD48

(Figure 1K), potently reduce the immunosuppressive phenotype of M-CSF macrophages derived from cultures in which IL-27 has been neutralized.

IL-27 neutralization during immunosuppressive macrophages generation alters their cellular metabolism

Inflammatory activation of mouse macrophages has been shown to result in reduced oxidative phosphorylation (OxPhos) and increased glycolysis, but it seems that this dichotomy is not so clear-cut in human macrophages.[32] Increasing evidence indicates that the metabolic programming of immune cells is an important determinant of their function.[33] We therefore studied the impact of IL-27 neutralization on macrophage metabolism. To determine whether the observed modifications were representative of a change in polarization, we first highlighted the differences between two macrophage populations classically considered to represent pro-inflammatory macrophages (monocytes differentiated with GM-CSF[7]) and macrophages found in tumors (macrophages differentiated with M-CSF called untreated above).

The Seahorse XF Cell MitoStress assay was performed to determine how mitochondrial oxidative respiration, and the resultant ATP production, changes comparing M-CSF-differentiated macrophages (M-CSF macrophages) to GM-CSF-differentiated macrophages (GM-CSF macrophages). We observed that GM-CSF macrophages had significantly higher basal respiration (oxygen consumption in the resting state) (Figure 2A) and higher respiration coupled ATP production (Figure 2B), suggesting that GM-CSF macrophages are energetically more demanding than M-CSF macrophages. Surprisingly, this increase in respiration is not linked to an increase in maximal respiration (Figure 2C), suggesting that GM-CSF macrophages exploit more their mitochondrial function without having an increased mitochondrial capacity.

The glycolytic function of GM-CSF and M-CSF macrophages was measured using the Seahorse XF Glycolysis Stress test. GM-CSF macrophages showed significantly higher glycolysis rate and glycolytic capacity when compared to M-CSF macrophages (Figure 2D and 2E), Glycolytic capacity indicates the maximum amount of glycolysis that cells can perform acutely. In order to estimate the glycolytic activity of the cells, we analyzed the concentration of lactate, a classical byproduct of glucose metabolism, in

culture supernatants. Our results showed that GM-CSF macrophages produced significantly more lactate in the basal state (Figure 2F).

We next performed the same assays with macrophages obtained from cultures with the IL-27-neutralizing antibody or the control antibody. Our results showed that IL-27 neutralization significantly altered the basal metabolism of M-CSF macrophages. Mα27 showed greater mitochondrial metabolism (Figure 2G) and a trend for greater glycolytic activity (Figure 2H) compared to Miso cells, that resulted in significant increases in ATP (Figure 2I) and lactate (Figure 2J) production.

These results suggest that IL-27 neutralization during macrophage differentiation affects their cellular metabolism in a way that places Mα27 closer to the inflammatory GM-CSF macrophages.

IL-27 neutralization during immunosuppressive macrophage generation restores their ability to activate CD4$^+$ and CD8$^+$ T cells

The observed changes on the phenotype, secretome and cellular metabolism of the anti-IL-27-treated (Mα27) macrophages lead to the hypothesis that these changes could also have an effect on the macrophage effector functions. Also, we first focused on the impact of activated macrophage culture supernatants on the ability of activated CD8$^+$ T cells to secrete IFNγ, a key molecule in the orchestration of proinflammatory and antitumoral Th1 responses and a potent inducer of inflammatory gene expression by T cells and antigen presenting cells (APC).

Our results showed that, after 48 h of activation, CD8$^+$ cells cultured in the presence of 10% (v:v) culture supernatant of activated M-CSF macrophages have almost completely inhibited IFNγ secretion compared to T cells cultured in the absence of supernatant (Supplementary Figure 3). Interestingly, under the same conditions, CD8$^+$ cells cultured with same volume of added Mα27 culture supernatant, secrete significantly more IFNγ than T cells cultured in the presence of Miso culture supernatant (Figure 3A).

To investigate the effect of Mα27 on the cytotoxic capacity of CD8$^+$ cells, we used an in vitro cytotoxicity model of co-incubation of a Muc-1 antigen-specific CD8$^+$ T clone, a luciferase-expressing mesothelioma cell line (Meso34) expressing Muc-1 and macrophages for 72 h.[34] The concentration of luciferase in the media, reflecting the 'killing' of tumor cells by the CD8$^+$ T cells, has been estimated using a luciferase substrate. Mα27 supernatant did not decrease CD8$^+$ T cell cytotoxicity, whereas Miso

supernatant decreased it by about 17%, compared to the condition without macrophages (Figure 3B). These results show that IL-27 neutralization during macrophage differentiation leads to macrophages that, unlike Miso, do not inhibit the cytotoxic activity of $CD8^+$ T cells.

For an optimal $CD8^+$ T cell response, it is necessary for $CD4^+$ T cells to secrete IL-2. Therefore, we evaluated the ability of culture supernatants from activated macrophages to modulate IL-2 secretion by $CD4^+$ T cells. The addition of 10% culture supernatant from activated macrophages significantly alters IL-2 secretion by $CD4^+$ cells. Specifically, after 48 h of activation, $CD4^+$ cells secreted twice as much IL-2 in the presence of culture supernatant from activated Mα27 compared with cells cultured in the presence of supernatant from Miso (Figure 3C). Based on this result, we evaluated the effect of activated macrophage culture supernatant on the proliferative capacity of $CD4^+$ T cells activated with anti-CD3 and anti-CD28 agonist antibodies. We found that activated Mα27 supernatant reduced the $CD4^+$ T cell replication index (shown as 0 for the condition without any macrophage supernatant) significantly less compared to activated untreated or Miso supernatant (Figure 3D). These results suggest that IL-27 neutralization during macrophage differentiation decreases their regulatory capacity.

In vivo neutralization of IL-27 delays tumor growth

With regard to the in vitro results and based on the described properties of IL-27 on immune cells[16,18,20,35–37], we investigate the impact of IL-27 neutralization on the establishment of a more antitumoral microenvironment using an in vivo tumor mouse model. A murine IL-27-neutralizing antibody was injected every two days in the subcutaneously implanted MC38 tumor, a commonly used murine model for colorectal carcinoma (Figure 4A). We observed that treatment with the IL-27-neutralizing antibody resulted in a significant delay of tumor growth after 10 days of treatment (Figure 4B) compared to mice injected with a non-relevant antibody (Figure 4C). Analysis of tumor growth curves showed that injection of the IL-27-neutralizing antibody significantly reduced tumor size as early as 6 days after the start of treatment (Figure 4D).

Furthermore, animals receiving IL-27-neutralizing antibody had a significantly better prognosis than animals receiving the control antibody, with a median survival of 18.5 vs. 14 days respectively, and a p-value of 0.008 (logrank test) (Figure 4F).

These results suggest that IL-27 neutralization in the TME decreases tumor growth rate and enables longer survival.

In vivo neutralization of IL-27 modifies the phenotype of tumor-infiltrating immune cells

To understand how IL-27 neutralization induced a decrease in the tumor growth rate, we analyzed CD39 expression on tumor-infiltrating immune cells at the end of treatment (day 10) (Supplementary Figure 4). Overall, treatment reduced CD39 expression levels in all myeloid cells (neutrophils, DC and newly recruited monocytes (still expressing Ly6C) and macrophages) (Figure 5A). This decrease was significant for newly recruited monocytes (Figure 5B), dendritic cells (Figure 5C) and neutrophils (Figure 5D).

There was also a significantly lower level of CD39 expression on $CD8^+$ T cells after treatment (Figure 5E). This appears to be related to a significant decrease in the percentage of CD39-expressing $CD8^+$ T cells (Figure 5F).

Concerning $CD4^+$ T cells, there was not a significant decrease in CD39 expression level for the whole population (Figure 5G), but the decrease was significant for those $CD4^+$ T cells highly expressing CD39 (Figure 5H), without any change in the percentage of cells expressing CD39 (Figure 5I).

These results demonstrate the value of IL-27 neutralization for increasing T cell efficacy in tumors.

Discussion

Here, we established the phenotypic, metabolic and functional changes induced by IL-27 neutralization during macrophage differentiation and the beneficial impact of IL-27 neutralization on tumor growth in vivo. In this work, we have shown that IL-27, a cytokine with both pro- and anti-inflammatory properties,[38–40] can enhance the immunoregulatory phenotype of macrophages obtained after culture under conditions allowing the differentiation of TAM-like macrophages.[22] Macrophages derived from IL-27-neutralized cultures (Mα27) showed an intermediate phenotype, with decreased expression of protumoral molecules and an increased expression of antitumoral ones. All these phenotypic changes are reflected in their functionality resulting in reduced inhibition of T lymphocyte functions. The results obtained from infiltrated $CD8^+$ T cells indicate a possible decrease in their exhaustion status, likely

associated to an increase in the duration of their functional capacity, while the results from $CD4^+$ T cells indicate a decrease in the level of CD39 at their surface, which could lead to a reduction in their regulatory activity.

CD39 is the molecule at the forefront of the adenosinergic pathway and is now considered as a key target in tumor control,[41] crucial for the polarization of immunoregulatory leukocytes[42] and implicated in cancer cell proliferation, survival and tumor metastasis.[43] It is an exhaustion marker generally co-expressed with inhibitory receptors.[44] CD39/CD73/A2AR targeting is currently the subject of over 50 clinical trials for the treatment of cancer.[41] Given the importance of CD39 in the maintenance of homeostasis in many functions,[45,46] it makes sense to investigate modulation CD39 via molecules less involved in homeostasis. In view of our results, we believe that IL-27 could be one such molecule.

Although IL-27 may have interesting properties in the fight against tumors,[20,39,47] in situations where the tumor microenvironment is highly immunosuppressive IL-27 seems to be rather deleterious. In this way, Park et al showed that IL-27 induces CD39 expression on tumor-infiltrating T cells with regulatory properties.[35]

In the in vivo part of our work, we showed that IL-27 neutralization during tumor progression resulted in delayed tumor growth which increases survival time and modulation of CD39 expression by tumor-infiltrating leucocytes.

These data provide preclinical relevant proof-of-principle for the utility of IL-27 targeting, and its potential interest in combination with PD-L1 blockade. We tested this hypothesis by assaying combined IL-27 neutralization and ICI treatment with anti-PD-L1 antibody in vivo in our tumor model (Supplementary Figure 5A). We showed that indeed prior IL-27 neutralization appeared to reduce tumor size compared to anti-PD-L1 treatment alone (Supplementary Figure 5B), leading to longer animal survival (Supplementary Figure 5C).

Our work suggests that IL-27 neutralization exerts a direct effect on the phenotype and function of macrophages, $CD8^+$ and $CD4^+$ T cells, affecting the TME and the tumor growth rate, while ultimately resulting in longer survival time. These properties make it a promising therapeutic target and could be of interest in modulating the tumor microenvironment prior to ICI treatment.

Acknowledgements

We thank all members of mice core facilities (UMS006, ANEXPLO, Inserm, Toulouse) for their support and technical assistance. We thank Dominique Rozet for the daily help on the administrative and financial management of our team. The authors are grateful to the CRCI2NA technical platforms for the support and to the We-Met platform for the Seahorse analysis. Flow cytometry experiments were done at the INFINITy-INSERM UMR1291 core facility connected to the Toulouse Réseau Imagerie network, member of the France-BioImaging national infrastructure supported by the French National Research Agency (ANR-10-INBS-04). We thank all team members for their availability and help.

Declaration of interest

None

Data Availability

The data that support the findings of this study are available from the corresponding author, [JT] upon reasonable request.

References

1. Lei, Q., Wang, D., Sun, K., Wang, L. & Zhang, Y. Resistance Mechanisms of Anti-PD1/PDL1 Therapy in Solid Tumors. *Front Cell Dev Biol* **8**, 672 (2020).
2. Kluger, H. M. *et al.* Defining tumor resistance to PD-1 pathway blockade: recommendations from the first meeting of the SITC Immunotherapy Resistance Taskforce. *J Immunother Cancer* **8**, e000398 (2020).
3. Nengroo, M. A., Verma, A. & Datta, D. Cytokine chemokine network in tumor microenvironment: Impact on CSC properties and therapeutic applications. *Cytokine* **156**, 155916 (2022).
4. Babar, Q., Saeed, A., Tabish, T. A., Sarwar, M. & Thorat, N. D. Targeting the tumor microenvironment: Potential strategy for cancer therapeutics. *Biochimica et Biophysica Acta (BBA) - Molecular Basis of Disease* **1869**, 166746 (2023).
5. Mantovani, A., Allavena, P., Marchesi, F. & Garlanda, C. Macrophages as tools and targets in cancer therapy. *Nat Rev Drug Discov* **21**, 799–820 (2022).
6. Bied, M., Ho, W. W., Ginhoux, F. & Blériot, C. Roles of macrophages in tumor development: a spatiotemporal perspective. *Cell Mol Immunol* **20**, 983–992 (2023).
7. Kerneur, C., Cano, C. E. & Olive, D. Major pathways involved in macrophage polarization in cancer. *Frontiers in Immunology* **13**, (2022).
8. Christofides, A. *et al.* The complex role of tumor-infiltrating macrophages. *Nat Immunol* **23**, 1148–1156 (2022).
9. Li, M., He, L., Zhu, J., Zhang, P. & Liang, S. Targeting tumor-associated macrophages for cancer treatment. *Cell & Bioscience* **12**, 85 (2022).
10. Argyle, D. & Kitamura, T. Targeting Macrophage-Recruiting Chemokines as a Novel Therapeutic Strategy to Prevent the Progression of Solid Tumors. *Frontiers in immunology* **9**, (2018).
11. Bejarano, L., Jordão, M. J. C. & Joyce, J. A. Therapeutic Targeting of the Tumor Microenvironment. *Cancer Discovery* **11**, 933–959 (2021).
12. Ries, C. H. *et al.* Targeting Tumor-Associated Macrophages with Anti-CSF-1R Antibody Reveals a Strategy for Cancer Therapy. *Cancer Cell* **25**, 846–859 (2014).
13. Kowal, J., Kornete, M. & Joyce, J. A. Re-education of macrophages as a therapeutic strategy in cancer. *Immunotherapy* **11**, 677–689 (2019).
14. van Dalen, F. J., van Stevendaal, M. H. M. E., Fennemann, F. L., Verdoes, M. & Ilina, O. Molecular Repolarisation of Tumour-Associated Macrophages. *Molecules* **24**, (2018).
15. Jeught, K. V. der *et al.* Targeting the tumor microenvironment to enhance antitumor immune responses. *Oncotarget* **6**, 1359–1381 (2014).
16. Alameddine, J. *et al.* Faecalibacterium prausnitzii Skews Human DC to Prime IL10-Producing T Cells Through TLR2/6/JNK Signaling and IL-10, IL-27, CD39, and IDO-1 Induction. *Front Immunol* **10**, (2019).
17. d'Almeida, S. M. *et al.* The ecto-ATPDase CD39 is involved in the acquisition of the immunoregulatory phenotype by M-CSF-macrophages and ovarian cancer tumor-associated macrophages: Regulatory role of IL-27. *Oncoimmunology* **5**, (2016).
18. Mascanfroni, I. D. *et al.* Interleukin-27 acts on dendritic cells to suppress the T-cell response and autoimmunity by inducing the expression of ENTPD1 (CD39). *Nat Immunol* **14**, 1054–1063 (2013).

393 19. Chihara, N. *et al.* Induction and transcriptional regulation of the co-inhibitory gene module in T cells. *Nature* **558**, 454–459
394 (2018).
395 20. Carbotti, G. *et al.* IL-27 induces the expression of IDO and PD-L1 in human cancer cells. *Oncotarget* **6**, 43267–43280 (2015).
396 21. Achard, C. *et al.* Oncolytic measles virus induces tumor necrosis factor-related apoptosis-inducing ligand (TRAIL)-mediated
397 cytotoxicity by human myeloid and plasmacytoid dendritic cells. *Oncoimmunology* **6**, e1261240 (2016).
398 22. Duluc, D. *et al.* Tumor-associated leukemia inhibitory factor and IL-6 skew monocyte differentiation into tumor-associated
399 macrophage-like cells. *Blood* **110**, 4319–4330 (2007).
400 23. Montalbán Del Barrio, I. *et al.* Adenosine-generating ovarian cancer cells attract myeloid cells which differentiate into adenosine-
401 generating tumor associated macrophages - a self-amplifying, CD39- and CD73-dependent mechanism for tumor immune escape.
402 *J Immunother Cancer* **4**, 49 (2016).
403 24. Zhou, R. *et al.* CD155 and its receptors in cancer immune escape and immunotherapy. *Cancer Letters* **573**, 216381 (2023).
404 25. Marin-Acevedo, J. A. *et al.* Next generation of immune checkpoint therapy in cancer: new developments and challenges. *J Hematol*
405 *Oncol* **11**, (2018).
406 26. Solomon, B. L. & Garrido-Laguna, I. TIGIT: a novel immunotherapy target moving from bench to bedside. *Cancer Immunol*
407 *Immunother* **67**, 1659–1667 (2018).
408 27. Kučan Brlić, P. *et al.* Targeting PVR (CD155) and its receptors in anti-tumor therapy. *Cell Mol Immunol* **16**, 40–52 (2019).
409 28. Mori, K., Hiroi, M., Shimada, J. & Ohmori, Y. Infiltration of M2 Tumor-Associated Macrophages in Oral Squamous Cell Carcinoma
410 Correlates with Tumor Malignancy. *Cancers* **3**, 3726 (2011).
411 29. Ara, A., Ahmed, K. A. & Xiang, J. Multiple effects of CD40–CD40L axis in immunity against infection and cancer. *Immunotargets*
412 *Ther* **7**, 55–61 (2018).
413 30. Take, Y., Koizumi, S. & Nagahisa, A. Prostaglandin E Receptor 4 Antagonist in Cancer Immunotherapy: Mechanisms of Action.
414 *Front Immunol* **11**, (2020).
415 31. Foucher, E. D. *et al.* IL-34- and M-CSF-induced macrophages switch memory T cells into Th17 cells via membrane IL-1α. *Eur J*
416 *Immunol* **45**, 1092–1102 (2015).
417 32. Vijayan, V. *et al.* Human and murine macrophages exhibit differential metabolic responses to lipopolysaccharide - A divergent
418 role for glycolysis. *Redox Biology* **22**, 101147 (2019).
419 33. Koo, S.-J. & Garg, N. Metabolic programming of macrophage functions and pathogens control. *Redox Biology* **24**, 101198 (2019).
420 34. Roulois, D. *et al.* Recognition of pleural mesothelioma by mucin-1(950–958)/human leukocyte antigen A*0201-specific CD8+ T-
421 cells. *European Respiratory Journal* **38**, 1117–1126 (2011).
422 35. Park, Y.-J. *et al.* IL-27 confers a protumorigenic activity of regulatory T cells via CD39. *Proc Natl Acad Sci U S A* **116**, 3106–3111
423 (2019).
424 36. Xia, S. *et al.* A requirement of dendritic cell-derived interleukin-27 for the tumor infiltration of regulatory T cells. *Journal of*
425 *Leukocyte Biology* **95**, 733–742 (2014).
426 37. Gerhardt, L., Hong, M. M. Y., Yousefi, Y., Figueredo, R. & Maleki Vareki, S. IL-12 and IL-27 Promote CD39 Expression on CD8+ T
427 Cells and Differentially Regulate the CD39+CD8+ T Cell Phenotype. *J Immunol* **210**, 1598–1606 (2023).
428 38. Aparicio-Siegmund, S. & Garbers, C. The biology of interleukin-27 reveals unique pro- and anti-inflammatory functions in
429 immunity. *Cytokine & Growth Factor Reviews* **26**, 579–586 (2015).

39. Liao, K.-L., Bai, X.-F. & Friedman, A. IL-27 in combination with anti-PD-1 can be anti-cancer or pro-cancer. *Journal of Theoretical Biology* **579**, 111704 (2024).

40. Villarino, A. V., Huang, E. & Hunter, C. A. Understanding the Pro- and Anti-Inflammatory Properties of IL-271. *The Journal of Immunology* **173**, 715–720 (2004).

41. Xia, C., Yin, S., To, K. K. W. & Fu, L. CD39/CD73/A2AR pathway and cancer immunotherapy. *Mol Cancer* **22**, 44 (2023).

42. Zhao, H., Bo, C., Kang, Y. & Li, H. What Else Can CD39 Tell Us? *Front. Immunol.* **8**, (2017).

43. Antonioli, L., Blandizzi, C., Pacher, P. & Haskó, G. Immunity, inflammation and cancer: a leading role for adenosine. *Nat Rev Cancer* **13**, 842–857 (2013).

44. Canale, F. P. *et al.* CD39 Expression Defines Cell Exhaustion in Tumor-Infiltrating CD8+ T Cells. *Cancer Research* **78**, 115–128 (2018).

45. PINSKY, D. J. CD39 AS A CRITICAL ECTONUCLEOTIDASE DEFENSE AGAINST PATHOLOGICAL VASCULAR REMODELING. *Trans Am Clin Climatol Assoc* **129**, 132–139 (2018).

46. Enjyoji, K. *et al.* Deletion of Cd39/Entpd1 Results in Hepatic Insulin Resistance. *Diabetes* **57**, 2311–20 (2008).

47. Hu, A. *et al.* Intra-Tumoral Delivery of IL-27 Using Adeno-Associated Virus Stimulates Anti-tumor Immunity and Enhances the Efficacy of Immunotherapy. *Front. Cell Dev. Biol.* **8**, (2020).

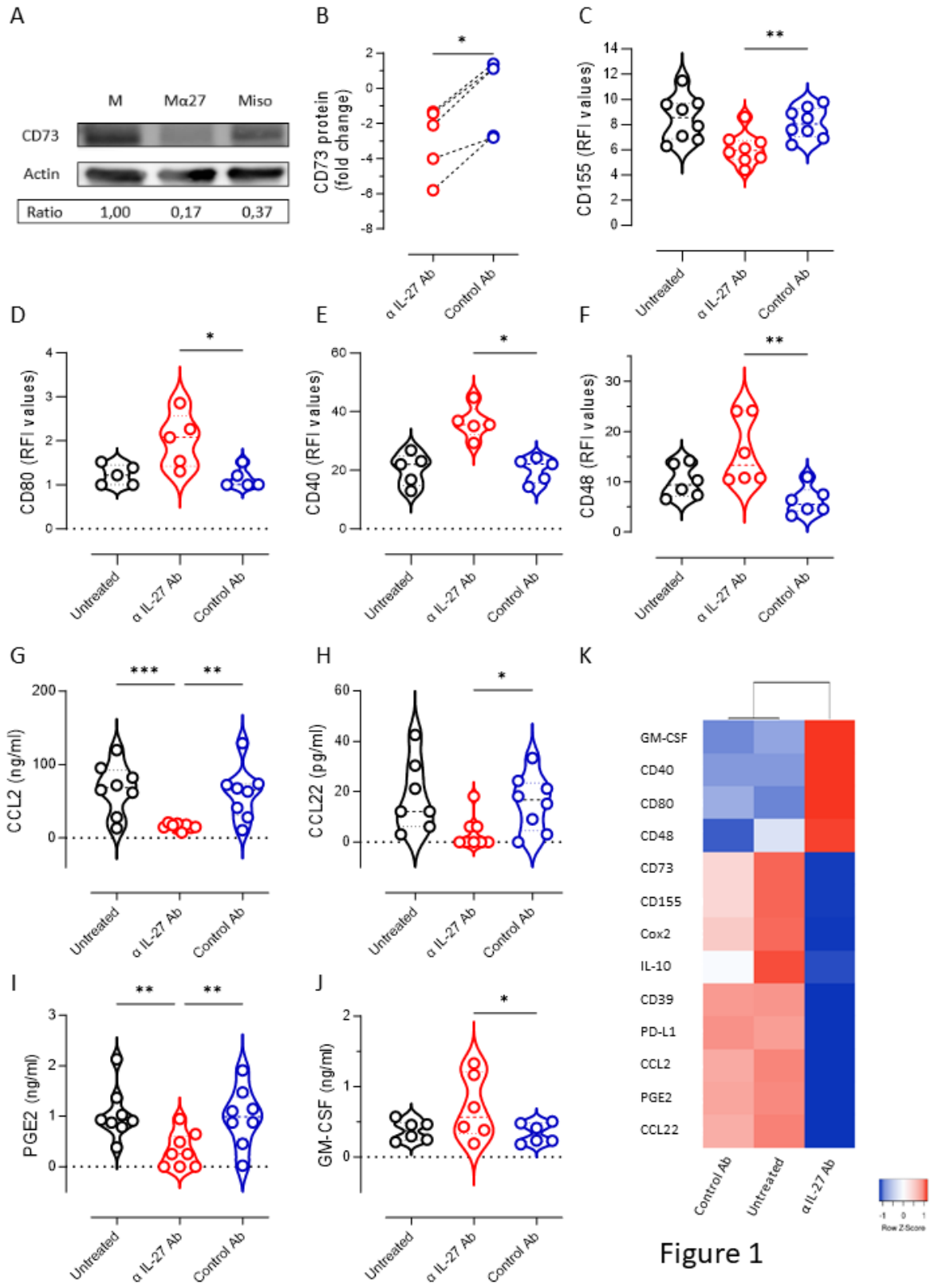
A
M
Mα27
Miso
CD73
Actin
Ratio
1,00
0,17
0,37
B
CD73 protein (fold change)
α IL-27 Ab
Control Ab
C
CD155 (RFI values)
Untreated
α IL-27 Ab
Control Ab
D
CD80 (RFI values)
E
CD40 (RFI values)
F
CD48 (RFI values)
G
CCL2 (ng/ml)
H
CCL22 (pg/ml)
I
PGE2 (ng/ml)
J
GM-CSF (ng/ml)
K
GM-CSF
CD40
CD80
CD48
CD73
CD155
Cox2
IL-10
CD39
PD-L1
CCL2
PGE2
CCL22
Control Ab
Untreated
α IL-27 Ab
Row Z-Score

Figure 1

462

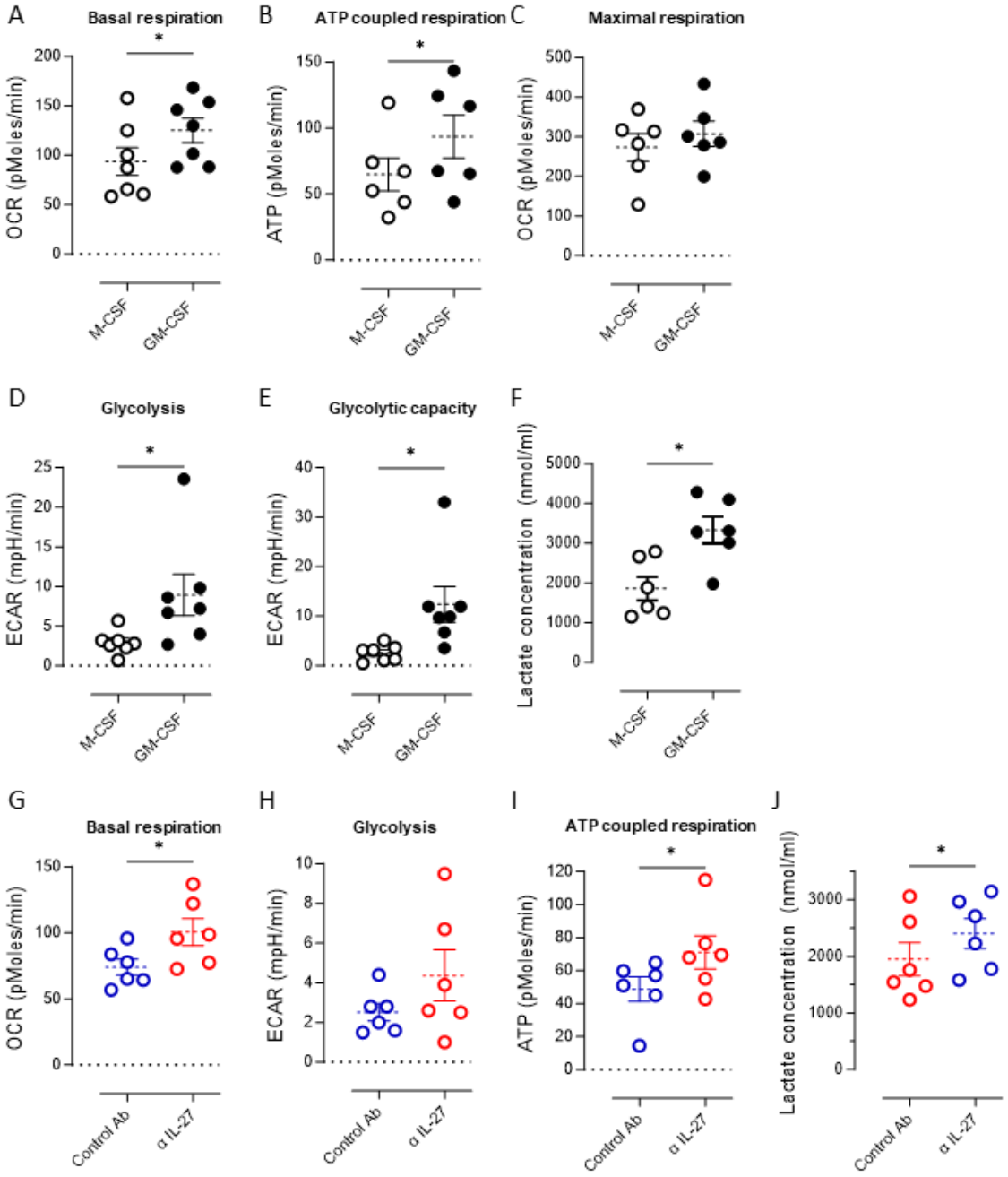
A
Basal respiration
OCR (pMoles/min)
M-CSF
GM-CSF
B
ATP coupled respiration
ATP (pMoles/min)
C
Maximal respiration
D
Glycolysis
ECAR (mpH/min)
E
Glycolytic capacity
F
Lactate concentration (nmol/ml)
G
Basal respiration
Control Ab
α IL-27
H
Glycolysis
I
ATP coupled respiration
J

Figure 2

463

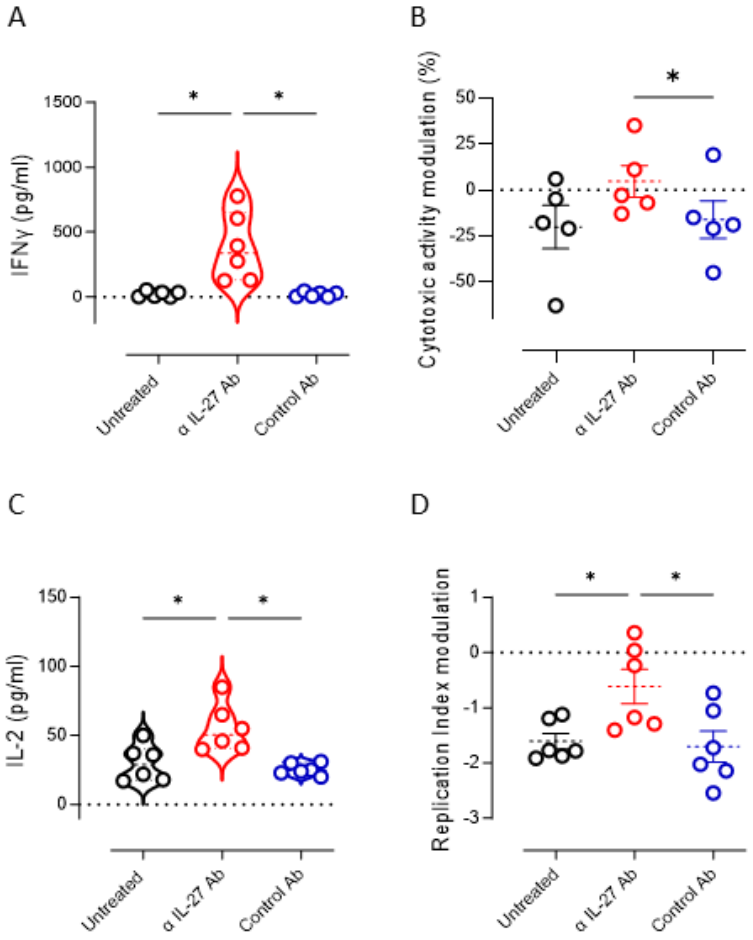
A
IFNγ (pg/ml)
1500
1000
500
0
*
*
Untreated
α IL-27 Ab
Control Ab
B
Cytotoxic activity modulation (%)
50
25
0
-25
-50
*
Untreated
α IL-27 Ab
Control Ab
C
IL-2 (pg/ml)
150
100
50
0
*
*
Untreated
α IL-27 Ab
Control Ab
D
Replication Index modulation
1
0
-1
-2
-3
*
*
Untreated
α IL-27 Ab
Control Ab

Figure 3

464

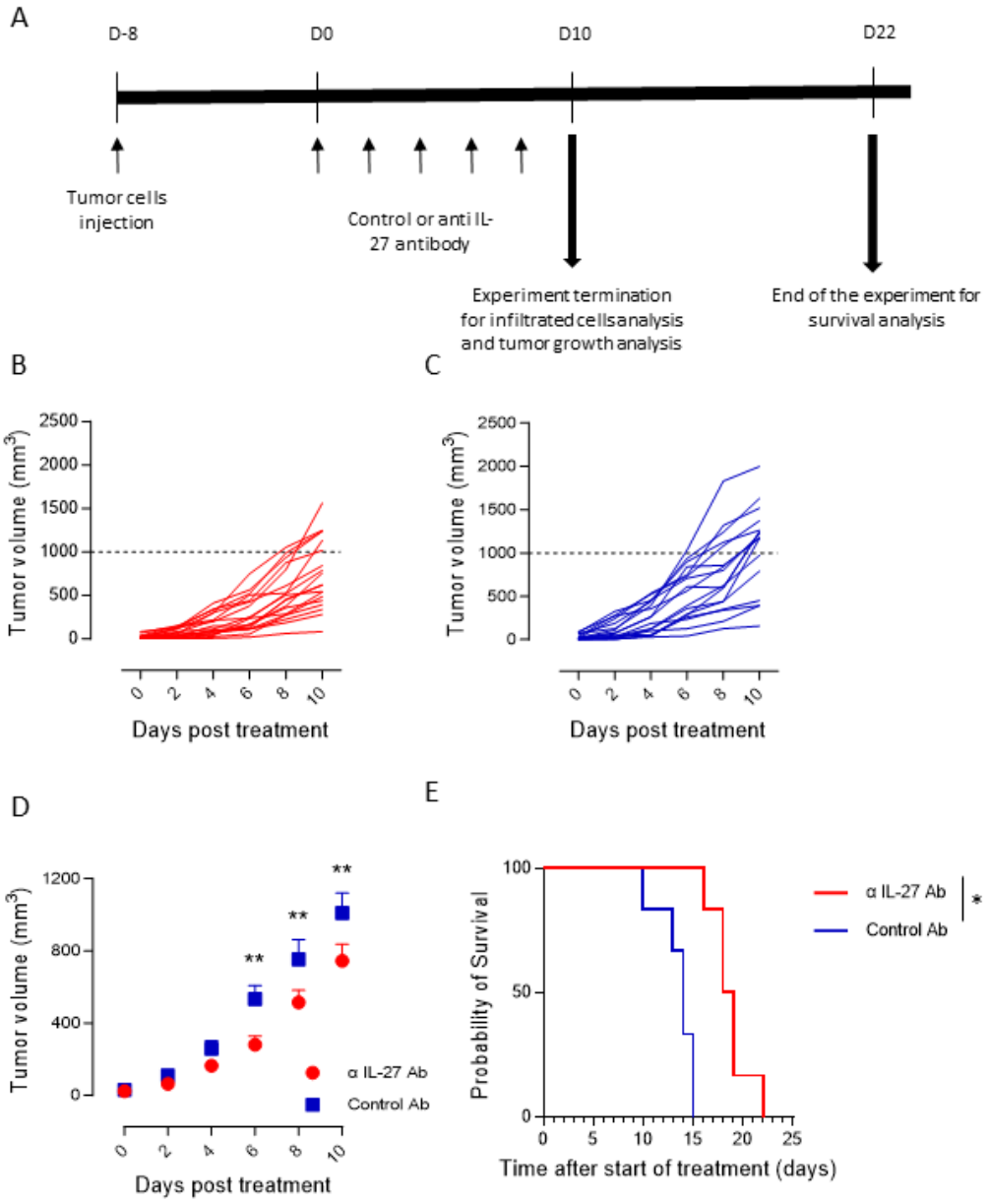
A
D-8
D0
D10
D22
Tumor cells injection
Control or anti IL-27 antibody
Experiment termination for infiltrated cells analysis and tumor growth analysis
End of the experiment for survival analysis
B
Tumor volume (mm3)
Days post treatment
C
Tumor volume (mm3)
Days post treatment
D
Tumor volume (mm3)
α IL-27 Ab
Control Ab
Days post treatment
E
Probability of Survival
α IL-27 Ab
Control Ab
Time after start of treatment (days)

Figure 4

465

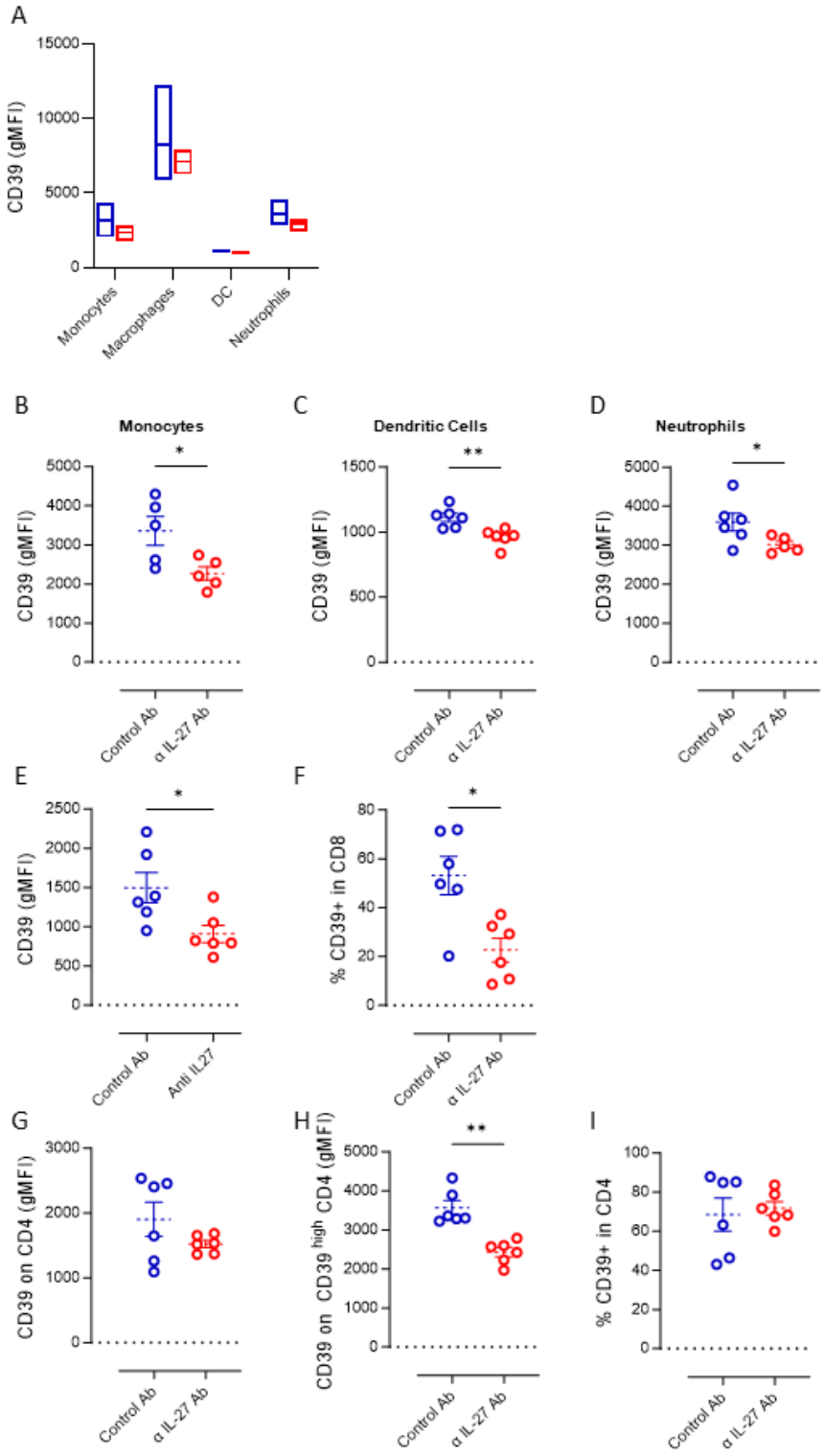

Figure 5

466

467

468

469

Figure Captions

Figure 1: Neutralization of IL-27 during macrophage differentiation modifies their phenotype. The level of expression of immunosuppressive and immunostimulatory molecules was analyzed in macrophages obtained after 7 days of culture with M-CSF (untreated), M-CSF plus an IL-27-neutralizing antibody (α IL-27 Ab) or M-CSF plus an isotype-matching control antibody (Control Ab). **(A)** CD73 protein quantification by western blot of a representative donor. **(B)** Pairwise comparison of the impact of treatments on CD73 protein expression levels compared to untreated cells (Wilcoxon test). Expression level of immunomodulatory molecules CD155 **(C),** CD80 **(D)**, CD40 **(E)**, CD48 **(F)** were analyzed by cytometry on $CD14^+$ gated cells. For each macrophage type, the concentration of CCL2 **(G)** and CCL22 **(H)** after 24 h of culture was quantified by ELISA. After macrophage stimulation (LPS) for 24hrs, the concentration of PGE2 **(I)** and GM-CSF **(J)** was analyzed by ELISA. **(K)** Heat map summarizing all the significant changes in macrophage phenotype induced by IL-27 neutralization.
All cytometry results are expressed in relative fluorescent intensity (RFI values are calculated from the ratio of MFI with antibody to MFI with isotype control antibody). RTqPCR results are expressed as mRNA expression normalized to GAPDH. ELISA results are expressed in ng/ml.
Each dot represents an independent experiment. Data are presented as mean ± SEM. Statistical analysis was performed with one-way ANOVA non-parametric tests, or as stated, using GraphPad Prism 10. Significance was considered for p values less than 0.05 (*p<0.05, **p<0.01, ***p<0.001).

Figure 2: Neutralization of IL-27 during macrophage differentiation affects their metabolic properties. (A-C) Scatter plot graphs comparing OCR parameters measured with Seahorse XF Cell Mito Stress Test: basal respiration, maximal respiration, and **respiration-linked ATP production** in macrophages differentiated with M-CSF or GM-CSF. **(D-E)** Scatter plot graphs comparing ECAR parameters measured with Seahorse XF Cell Glyco Stress Test: Glycolysis and Glycolytic Capacities in macrophages differentiated with M-CSF or GM-CSF. **(F)** Lactate concentration in macrophages differentiated with M-CSF or GM-CSF **(G and I)** Scatter plot graphs comparing OCR parameters measure with Seahorse XF Cell Mito Stress Test: basal respiration, and **respiration linked ATP production** in Miso and Mα27 macrophages. **(H)** Scatter plot graphs comparing ECAR parameters measured with Seahorse XF Cell Glyco Stress Test reflecting glycolysis in basal condition in Miso and Mα27 macrophages. **(J)** Lactate concentration in Miso and Mα27 macrophages. Each dot represents an independent experiment. Data are presented as mean values ± SEM. Statistical analysis was performed with two-tailed Student's *t* test, using GraphPad Prism 10. Significance was considered for p values less than 0.05 (*p<0.05).

Figure 3: Neutralization of IL-27 during macrophage differentiation restores their ability to activate T cells
IL-27 neutralization alters macrophage functional capabilities. Macrophages differentiated with M-CSF (Untreated), M-CSF plus IL-27-neutralizing antibody (α IL-27 Ab) or M-CSF plus control antibody (Control Ab) were activated in the presence of LPS. Culture medium (conditioned medium) and cells were recovered after 24 h. Secretion of **(A)** IFNγ by CD8+ T cells or **(C)** IL-2 by CD4+ T cells. IFNγ and IL-2 levels were quantified by ELISA. **(B)** Scatter plot showing the effect of macrophages on the cytotoxic capacity of a $CD8^+$ T clone. Macrophages differentiated with M-CSF (Untreated), M-CSF plus IL-27-neutralizing antibody (α IL-27 Ab) or M-CSF plus control antibody (Control Ab) were brought into contact with the $CD8^+$ T cells and the target tumor cells for 72 h. The impact on cytotoxicity is expressed as the percentage of change in cytotoxicity compared to the cytotoxicity measured in the absence of macrophages. **(D)** Scatter plot showing the impact of the respective conditioned media added (10% of the final volume) on the replication index of $CD4^+$ T cells. The $CD4^+$ replication index was analyzed, after 6 days of culture, by flow cytometry and revealed from the dilution of the intracytoplasmic marker CFDA-SE. Each dot represents an independent experiment. ELISA results are expressed in ng/mL. Data are presented as mean ± SEM. Statistical analysis was performed with one-way ANOVA non-parametric tests, using GraphPad Prism 10. Significance was considered for p values less than 0.05 (*p<0.05).

Figure 4: Therapeutic efficacy of anti-IL-27 antibody
(A) $5x10^5$ MC38 cells were injected subcutaneously in the right flank of C57BL/6 mice. Eight days post-injection (D0) they were treated with IL-27-neutralizing antibody or a non-relevant control antibody of the same isotype, every other day (D0, D2, D4, D6, D8). In total, treatment was injected five times intratumorally. The tumor volumes monitoring experiment was stopped when the first tumor reached 1800 mm3 (D10). The survival experiment was stopped when the last tumor reached 1800 mm3 (D22). Tumor volume has been measured from D0 to D10 and is depicted as spider plots according to the received treatment; **(B)** anti-IL-27 treatment and **(C)** control antibody. **(D)** Global curve showing cumulative tumor volumes every two days. **(E)** Scatter plot showing tumor volumes on days 0, 4 and 10 after treatment initiation. **(F)** Each mouse was sacrificed when the tumor mass reached a limit of 1800 mm^3. The graph shows the overall survival of M38 tumor-bearing mice according to the received treatment.
In all cases each data point represents a mouse. Data have been pooled from two independent repeats and are presented as mean ± SEM. Statistical analysis was performed with one-way ANOVA nonparametric tests, using GraphPad Prism 10. Significance was considered for p values less than 0.05 (*p<0.05, **p<0.01). For survival analysis, we used a logrank test with a p value of 0.008.

Figure 5: Effect of IL-27 neutralization on CD39 expression on tumor-infiltrating immune cells
Once MC38 tumors had reached 20-50 mm^3, i.e. around day 8 after tumor cell injection, mice received an intratumoral injection of IL-27-neutralizing or isotype control antibody every other day (D0, D2, D4, D6, D8). Mice were sacrificed on

day 10 after treatment initiation and the tumor mass was digested for cellular analysis. **(A)** Box plot showing CD39 gMFI on the indicated myeloid cell populations in MC38 tumors. The gMFI for neutrophils **(B)**, dendritic cells **(C)** and monocytes **(D)** is shown on scatter plots. **(E)** Scatter plot showing gMFI of CD39 on infiltrating $CD8^+$ T cells. **(F)** Quantitative analysis of $CD39^+CD8^+$ T lymphocytes from flow cytometry analysis. **(G)** Scatter plot showing gMFI of CD39 on infiltrating $CD4^+$ T cells. **(H)** Scatter plot showing gMFI of CD39 on infiltrating $CD4^+$ T cells strongly expressing CD39. **(I)** Quantitative analysis of $CD39^+CD4^+$ T cells by flow cytometry. In all cases each data point represents a mouse. Pooled data from two independent repeats are presented as mean ±SEM. Statistical analysis was performed with Mann–Whitney tests, using GraphPad Prism 10 software. Significance was considered for p values less than 0.05 (*$p<0.05$, **$p<0.01$).